

NAVAL POSTGRADUATE SCHOOL

Monterey, California



THESIS

INTERMODULATION IN CHANNELIZED DIGITAL ESM RECEIVERS

by

Cheng, Ming-Jen

September, 1996

Thesis Advisor:

D. C. Schleher

Approved for public release; distribution is unlimited.

DTIC QUALITY INSPECTED 1

19970123 041

REPORT DOCUMENTATION PAGE			Form Approved OMB No. 0704-0188	
Public reporting burden for this collection of information is estimated to average 1 hour per response, including the time for reviewing instruction, searching existing data sources, gathering and maintaining the data needed, and completing and reviewing the collection of information. Send comments regarding this burden estimate or any other aspect of this collection of information, including suggestions for reducing this burden, to Washington Headquarters Services, Directorate for Information Operations and Reports, 1215 Jefferson Davis Highway, Suite 1204, Arlington, VA 22202-4302, and to the Office of Management and Budget, Paperwork Reduction Project (0704-0188) Washington DC 20503.				
1. AGENCY USE ONLY (Leave blank)		2. REPORT DATE September 1996		3. REPORT TYPE AND DATES COVERED Master's Thesis
4. TITLE AND SUBTITLE INTERMODULATION IN CHANNELIZED DIGITAL ESM RECEIVERS			5. FUNDING NUMBERS	
6. AUTHOR(S) Cheng, Ming-Jen				
7. PERFORMING ORGANIZATION NAME(S) AND ADDRESS(ES) Naval Postgraduate School Monterey CA 93943-5000			8. PERFORMING ORGANIZATION REPORT NUMBER	
9. SPONSORING/MONITORING AGENCY NAME(S) AND ADDRESS(ES)			10. SPONSORING/MONITORING AGENCY REPORT NUMBER	
11. SUPPLEMENTARY NOTES The views expressed in this thesis are those of the author and do not reflect the official policy or position of the Department of Defense or the U.S. Government.				
12a. DISTRIBUTION/AVAILABILITY STATEMENT Approved for public release; distribution is unlimited.			12b. DISTRIBUTION CODE	
13. ABSTRACT (maximum 200 words) This thesis investigates intermodulation distortion generated by analog-to-digital converters (ADCs) in a channelized digital ESM receiver when processing multiple signals simultaneously. The spurious free dynamic range (SFDR) associated with this distortion is discussed. Two methods for increasing the spurious free dynamic range are evaluated. First, by adding a small amount of Gaussian noise to the input of the receiver, the intermodulation distortion is found to be reduced significantly. Second, by using a narrow bandwidth sub-Nyquist sampling rate with high dynamic range ADCs it is possible to increase the spurious free dynamic range of the digital receiver. The first method is a simple approach but the ability to increase the SFDR is limited. The second method is more effective but requires greater computation and complex receiver design.				
14. SUBJECT TERMS Intermodulation, Digital ESM Receivers			15. NUMBER OF PAGES 64	
			16. PRICE CODE	
17. SECURITY CLASSIFICATION OF REPORT Unclassified	18. SECURITY CLASSIFICATION OF THIS PAGE Unclassified	19. SECURITY CLASSIFICATION OF ABSTRACT Unclassified	20. LIMITATION OF ABSTRACT UL	

Approved for public release; distribution is unlimited.

INTERMODULATION IN CHANNELIZED DIGITAL ESM RECEIVERS

Cheng, Ming-Jen
Major, Republic of China Air Force
B.S., University of Tulsa, 1991

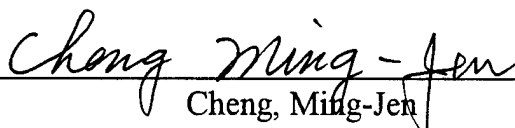
Submitted in partial fulfillment
of the requirements for the degree of

MASTER OF SCIENCE IN SYSTEMS ENGINEERING

from the

NAVAL POSTGRADUATE SCHOOL
September 1996

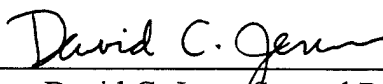
Author:


Cheng, Ming-Jen

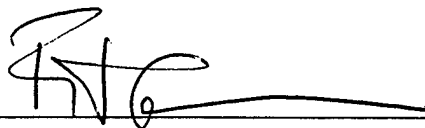
Approved by:



D. C. Schleher, Thesis Advisor



David C. Jenn, Second Reader



Frederic H. Levien, Chairman
Electronic Warfare Academic Group

ABSTRACT

This thesis investigates intermodulation distortion generated by analog-to-digital converters (ADCs) in a channelized digital ESM receiver when processing multiple signals simultaneously. Spurious free dynamic range (SFDR) associated with this distortion is discussed. Two methods for increasing spurious free dynamic range are evaluated. First, by adding a small amount of Gaussian noise to the input of the receiver, the intermodulation distortion is found to be reduced significantly. Second, by using a narrow bandwidth sub-Nyquist sampling rate with high dynamic range ADCs it is possible to increase the spurious free dynamic range of the digital receiver. The first method is a simple approach but the ability to increase the SFDR is limited. The second method is more effective but requires greater computation and complex receiver design.

TABLE OF CONTENTS

I.	INTRODUCTION	1
A.	CHANNELIZED DIGITAL ESM RECEIVER AND ANALOG-TO-DIGITAL CONVERTERS (ADC)	1
B.	THE EW ENVIRONMENT AND PULSE DENSITY	4
II.	FREQUENCY DOMAIN MEASUREMENT OF INTERMODULATION DISTORTION AND SPURIOUS FREE DYNAMIC RANGE	7
A.	SIMULATION OF A CHANNELIZED DIGITAL ESM RECEIVER	10
B.	SINGLE SIGNAL ANALYSIS	12
C.	TWO SIGNALS ANALYSIS	15
D.	MULTIPLE SIGNALS ANALYSIS	20
III.	REDUCTION IN INTERMODULATION DISTORTION DUE TO ADDITIVE NOISE	23
A.	ADDITIVE NOISE LEVEL AND INTERMODULATION DISTORTION	24
B.	ADDITIVE NOISE LEVEL AND SFDR	27
IV.	SUB-NYQUIST RATE APPROACH	29
V.	CONCLUSION	35
APPENDIX A	NYQUIST SAMPLING RATE SIMULATION FOR ONE INPUT SIGNAL	37
APPENDIX B	NYQUIST SAMPLING RATE SIMULATION FOR TWO INPUT SIGNALS	41
APPENDIX C	SUB-NYQUIST SAMPLING RATE SIMULATION FOR TWO INPUT SIGNALS	45
	LIST OF REFERENCES	49
	INITIAL DISTRIBUTION	51

LIST OF FIGURES

1. Performance of Current ADCs	2
2. Block Diagram of a Typical Channelized Digital ESM Receiver	3
3. Block Diagram of a Two-Channel Digital ESM Receiver	11
4. FFT Filters	12
5. ADC Output of a Digital Receiver with One Input Signal	13
6. IF Spectrum of a Digital Receiver with One Input Signal	14
7. IF Spectrum of a Digital Receiver with Two Input Signals	16
8. ADC Output of a Digital Receiver with Two Input Signals	17
9. A Third Input Signal Amplitude Below Peak Harmonic Level	19
10. IF Spectrum of a Digital Receiver with Fifteen Input Signals	20
11. Block Diagram of a Digital ESM Receiver with a Noise Source	23
12. The Output Spectrum (a) with or (b) without Additive Noise	25
13. Additive Noise verses Intermodulation Distortion	26
14. Additive Noise verses SINAD	26
15. Additive Noise verses SFDR	27
16. SFDR Test with a Third Input Signal	28
17. Basic Sub-Nyquist Sampling Structure of a Digital Receiver	30
18. The Comparison of Sub-Nyquist and Nyquist sampling Spectrum	32
19. SFDR Test for Two Different Sampling Schemes	33

LIST OF TABLES

1. Total Emitter and Pulse Density Figures	5
2. Dynamic Range and SNR vs. Number of ADC Bits	15
3. SFDR, SINAD, and IMD vs. Number of ADC Bits	19
4. SFDR and SINAD of an 8 bits ADC	21

I. INTRODUCTION

A. CHANNELIZED DIGITAL ESM RECEIVER AND ANALOG-TO-DIGITAL CONVERTERS (ADC)

Modern electronic support measures (ESM), or electronic support (ES), receivers require a wide instantaneous bandwidth and high dynamic range in order to receive and process multiple signals at the same time. Modern signals such as frequency agility radar may have a 500 MHz frequency hopping bandwidth or greater. It is impossible for a narrow band superheterodyne ESM receiver to tune to each frequency component of the frequency agility radar. However a channelized digital ESM receiver with a 500 MHz or higher instantaneous bandwidth using a fixed local oscillator frequency, can process all frequency components within its bandwidth by taking samples of in phase and quadrature sinusoid components from the output of an analog-to-digital converter (ADC) and utilizing the Fast Fourier Transform (FFT) to perform frequency domain analysis. This is accomplished without rapidly tuning the local oscillator frequency as occurs in a conventional narrow band superheterodyne receiver.

Spectral analysis techniques are the key to advanced receiver designs and provide an essential parameter for emitter sorting and also for the efficient allocation of ECM resources. Real-time digital spectrum analysis is possible using special hardware configured to accomplish the fast Fourier transform (FFT) algorithm. High speed multipliers and accumulators are currently available in large-scale integration (LSI) form, which can be linked together in pipeline structures to perform a complex FFT. A critical component which limits the use of a high speed digital processor is the analog-to-digital converter (ADC), which

translates the analog waveform at the input of the processor into a digital word that is manipulated in the processor. [Ref. 1]

Due to the rapid development of analog-to-digital converters (ADCs), building of wideband digital ESM receivers becomes a reality. Digital ESM receivers rely on high speed ADCs and digital signal processing techniques in order to encode the received signals into Pulse Description Words (PDW) in real time and store them into memory for future analysis and ECM functions. Figure 1 shows a survey on the capability of current ADCs. The information on the ADCs was obtained from [Ref. 2] through [Ref. 10].

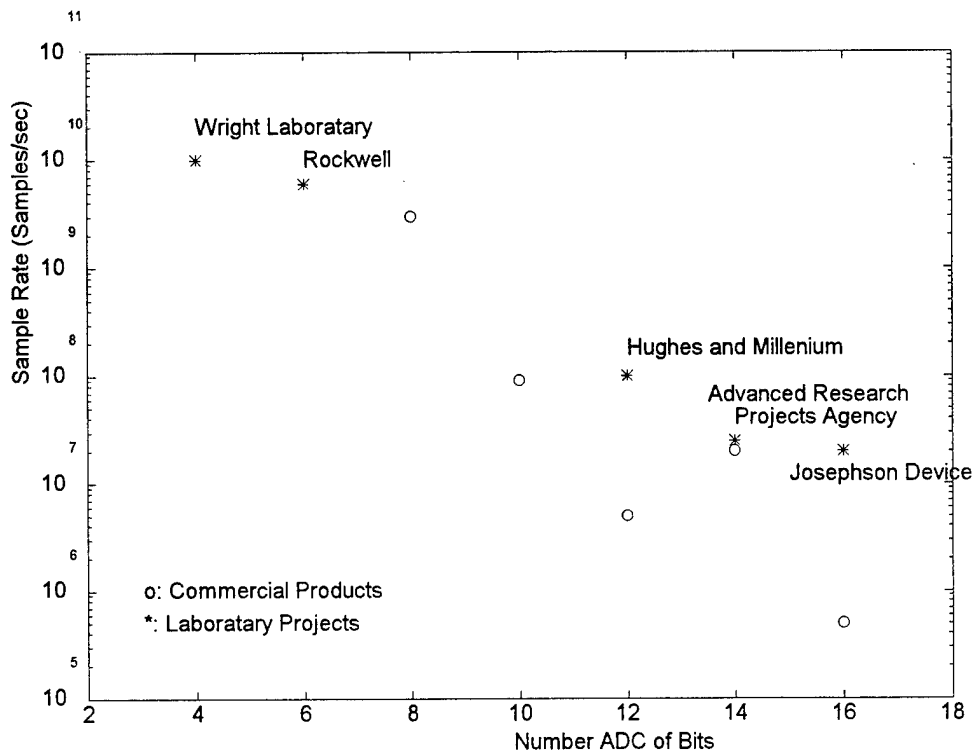


Figure 1. Performance of Current ADCs

A channelized digital ESM receiver can be represented in functional blocks as shown

in Figure 2. The output from the ADC is digital. These data are in the time domain and the information is available as spectral lines or spectrum density. However, these outputs do not completely satisfy ESM requirements. The spectral lines must be converted into carrier frequencies of the input signals. In order to emphasize this process, a parameter encoder is identified separately from the spectrum estimator. The parameter encoder converts the frequency information into the desired Pulse Description Words (PDW) [Ref. 10].

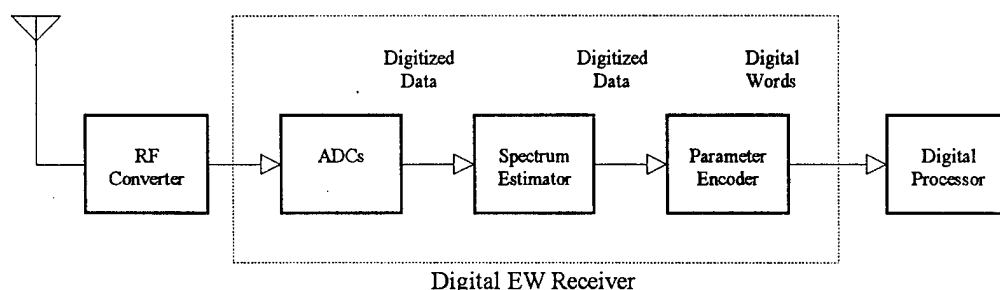


Figure 2. Block Diagram of a Typical Channelized Digital ESM Receiver

Since the channelized digital ESM receiver allows multiple radar signals to be down converted into IF components within the passband at the same time, intermodulation products appear at the ADC output and the receiver reports more signals than it has received. We can generally increase the threshold setting of the receiver to eliminate intermodulation products, but these will decrease the dynamic range of the receiver and lose weak signals. Sometimes the weak signals are the most important signals because they can come from weapon control radars or airborne fire control radars that are transmitted at low power levels intentionally to reduce the probability of being intercepted. The intermodulation products created by the ADC do not always behave as they do for linear devices where reduced input levels result in

predictable reductions in intermodulation products. We need to find other ways to reduce the intermodulation products and increase dynamic range to an acceptable level which is the objective of this thesis.

B. THE EW ENVIRONMENT AND PULSE DENSITY

According to the research done by Peot [Ref. 11], the worst case radio frequency (RF) electronic combat environment is a high-altitude aircraft conducting a mission over central Europe. Table 1 shows the total emitter and pulse density in the year 2000, which includes the signals from airborne intercept radars, ground-based SAM, ground-based AAA and other miscellaneous emitters. These figures are based on rough assumption in the year 2000 which may differ from the actual environment. The assumptions for the scenario are as follows:

- No more than 25% of the aircrafts are in the air at once for either side and 50% of the airborne interceptor radars are on all of the time.
- The average pulse repetition frequency (PRF) for ground-based or miscellaneous emitters is 200 Hz.
- The PRF for airborne fire control radar is 15 KHz.
- The receiver is assumed operating in noiseless environment.
- The terrain is flat.
- About 50% of the AAA system will be radar-guided.

From Table 1 we can see that there are several million samples per second for each type of emitter from each side. It is the number of pulses impinging on the aircraft. The

actual number of pulses received by the aircraft is scaled by the receiver sensitivity, terrain masking, receiver antenna coverage, look through percentage and other factors. As stated by Peot, using parallel architecture and high speed special purpose processing the EW system designer can achieve the processing densities required for the EW signal processors of the year 2000.

The probability of pulse overlaps will be high in the above scenario. A good channelized digital ESM receiver design should be able to reduce the intermodulation distortion which may occur in such environment.

Table 1. Total Emitter and Pulse Density Figures

Emitter	No. Of Emitter	% in LOS	% Active	Emitters Visible	Mainlobe Sidelobe Visibility(%)	Average PR	Pulse Density Contribution (Pulse per second)
NATO A/A Radar	1250	100	50	625	50	15000	4.7×10^6
Warsaw Pact A/A Radar	2000	100	50	1000	50	15000	7.5×10^6
NATO AAA	4250	50	100	2125	50	2000	2.1×10^6
Warsaw Pact AAA	2650	50	100	1325	50	2000	1.3×10^6
NATO SAM	4400	50	100	2200	50	2000	2.2×10^6
Warsaw Pact SAM	19000	50	100	9500	50	2000	9.5×10^6
Misc	1000			1000		2000	2.0×10^6
Total	34550	---	---	18000	---	---	29×10^6

II. FREQUENCY DOMAIN MEASUREMENT OF INTERMODULATION DISTORTION AND SPURIOUS FREE DYNAMIC RANGE

Channelized digital ESM receivers employ baseband and direct IF digitization which place stringent performance requirements on analog-to-digital converters (ADCs). Receiver performance is limited by the dynamic parameters of the ADC. We can derive the dynamic parameters using the Fast Fourier Transform (FFT). The MATLAB software provides unique FFT and FFTSHIFT functions which are convenient to use in digital receiver simulation. All the simulations and calculations in this thesis were done in MATLAB.

The input signal is set to be a 1V peak amplitude sine wave. The ADC simulation converts the 1V peak amplitude sine wave signal to its maximum response which means the maximum output of the ADC is also set to 1 V peak. Any analog input signal is rounded (or truncated) to its nearest digital code, the rounding (or truncating) error represents the quantization error in a real ADC. The analog input range is divided into 2^n digital codes so that each digital output code represents a corresponding analog input level within the quantization range. The FFT operation collects the digital codes and generates data for frequency domain evaluation.

The key frequency domain ADC specifications concerning this thesis are signal-to-noise-ratio (SNR), total harmonic distortion (THD), dynamic range (DR), intermodulation distortion (IMD), signal-to-noise plus distortion (SINAD), and spurious free dynamic range (SFDR) which can be obtained from the FFT operation.

The most important dynamic specification of a converter is the signal-to-noise ratio

(SNR). The SNR is related to the quantization noise power of the ADC, which determines the sensitivity level of the receiver. The formula for calculating the maximum SNR for an ideal ADC is $6.02n+1.76$ dB where n is the number of quantization bits [Ref. 10]. SNR measures signal power relative to noise power which is appropriate to single input signal analysis. We can calculate the actual noise power from the FFT output. SNR as applied to a single signal would be calculated as

$$SNR = 10 \log \left(\frac{P_{signal}}{\sum P_{noise}} \right) \text{ dB} \quad (1)$$

where P_{signal} is the power of the input signal after FFT processing and P_{noise} is the sum of all quantization noise after FFT processing, or, equivalently, by removing the carrier and harmonic components from normalized FFT spectrum (set the ideal full-scale spectrum level to 1) and calculate the RMS values of the remaining points. Since the SNR is in positive decibels, negative sign is needed. We can simplify the Equation 1 as:

$$SNR = -10 \log (\sum P_{noise}) \text{ dB} \quad (2)$$

For example, if there are 512 samples in the normalized FFT spectrum, then we can remove the carrier sample and sum up the remaining 511 quantization noise samples to obtain the SNR without considering the carrier amplitude since it has been normalized to 1. The rest of the dynamic specifications may follow this principle.

THD measures the total power at the harmonic distortion frequencies $P_{harmonics}$ by removing the carrier and noise components from the normalized FFT spectrum and calculating the RMS values of the remaining points. THD is given by the following form:

$$THD=10\log(\sum P_{harmonics}) \text{ dB} \quad (3)$$

IMD measures the total power at the intermodulation distortion frequencies by removing the carrier signals, harmonics, and noise from the normalized FFT spectrum and calculating the RMS values of the remaining points. IMD is given by the following form:

$$IMD=10\log(\sum P_{intermods}) \text{ dB} \quad (4)$$

SINAD measures the total power at the harmonic distortion frequencies and noise by removing the carrier signals from the normalized FFT spectrum and calculating the RMS values of the remaining points. This is more appropriate when analyzing multiple input signals. SINAD is given by

$$SINAD=10\log(\sum P_{harmonics} + \sum P_{noise} + \sum P_{intermods}) \text{ dB} \quad (5)$$

There are three different types of dynamic range we need to consider for evaluating the performance of an ADC:

- Single signal dynamic range (DR):

DR measures the power ratio of the strongest signal that the receiver can properly detect without generating spurious responses to the signal at the receiver's sensitivity level. This is equal to the signal-to-noise ratio (SNR) of the system measured over a bandwidth equal to half the sampling frequency.

- Spurious free dynamic range (SFDR):

SFDR relates to the third-order intermodulation or harmonic distortions which

measures the power ratio of the strongest signal that the receiver can properly encode without generating detectable third-order intermodulation or harmonic distortions to the power at the noise level. It is equal to the ratio between the maximum signal component and the largest distortion component that can be obtained.

- Instantaneous dynamic range (IDR):

IDR measures the power ratio of the maximum and minimum simultaneous received pulses that can be properly encoded by the receiver.

The three different types of dynamic ranges can be calculated from the normalized results after FFT processing by using the following equations:

$$DR \approx SNR \quad (6)$$

$$SFDR = -10 \log (\text{Peak Harmonic or Intermod Power}) \quad (7)$$

$$IDR = -10 \log (\text{Peak Weakest Signal Power}) \quad (8)$$

A. SIMULATION OF A CHANNELIZED DIGITAL ESM RECEIVER

Figure 3 shows the basic simulation structure of a channelized wideband digital ESM receiver using the two-channel approach. The passband ($H_{BP}(f)$) of the receiver is designed from 1000 MHz to 1500 MHz which can detect the lower-half of L-band search radar signals. The input signal passes through a bandpass filter and a 90 degree hybrid divides the input signal into in-phase (I channel) and quadrature-phase (Q channel) channels. The local oscillator generates 1250 MHz sine wave signal that feeds directly to the I channel and the Q channel mixers. The mixers down convert the input signals into two baseband video

signals. The I and Q signals feed two separate lowpass filters. The cutoff frequency of the lowpass filters ($H_{LP}(f)$) is 250 MHz. The bandwidth of the receiver equals the sampling rate of the I-Q channel ADC. The ADCs digitize the IF signals into binary codes with maximum response to the input signal. Since the I-Q outputs are both digitized, the information content of the input signal is essentially doubled.

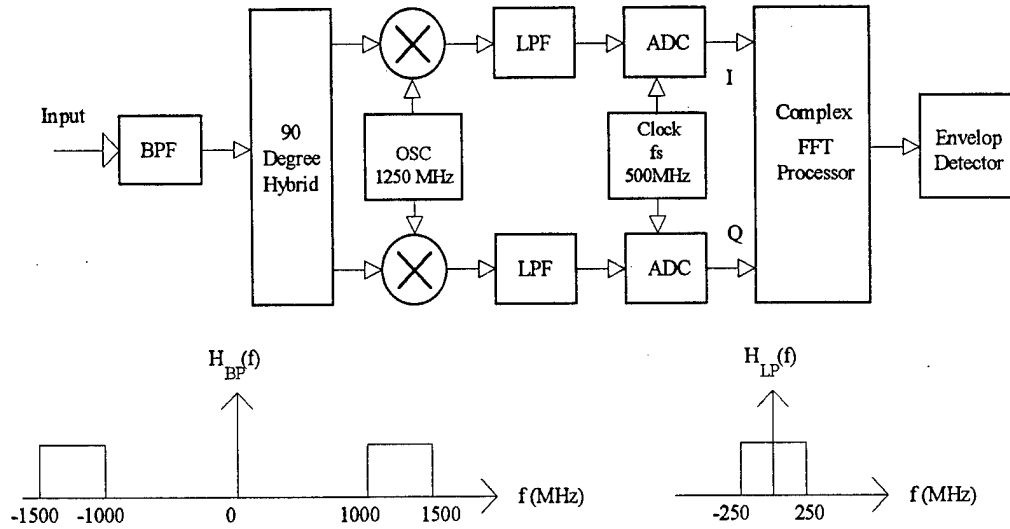


Figure 3. Block Diagram of a Two-Channel Digital ESM Receiver

For a N point FFT with sampling rate equal to half of the Nyquist rate $f_s = f_N/2$, the frequency resolution ΔF for each FFT bin would be:

$$\Delta F = \frac{f_s}{N} \quad (9)$$

The bandwidth (BW) of a two-channel digital ESM receiver equals the sampling rate f_s :

$$BW = f_s \quad (10)$$

The N point FFT functions as N bandpass filters, each FFT bin covers a frequency band as

shown on Figure 4.

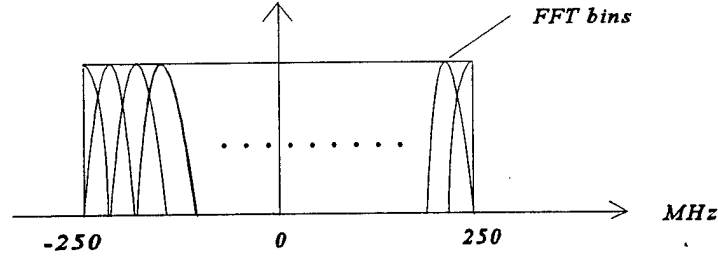


Figure 4. FFT Filters

B. SINGLE SIGNAL ANALYSIS

The simulation is done by using a 1 V peak amplitude sine wave signal $\sin(2\pi f_i t)$ as an input signal to the receiver. The in-phase local oscillator signal is $2\sin(2\pi f_o t)$ which directly feeds to the I channel mixer, while the Q channel mixer signal is $2\sin(2\pi f_o t + 90^\circ)$ or $2\cos(2\pi f_o t)$. In order to simplify the simulation, we only consider the frequency components below 250 MHz and neglect the effects of the lowpass filters. The outputs from the I and Q channel become:

$$\begin{aligned} I(t) &= \sin(2\pi f_i t) \cdot 2\sin(2\pi f_o t) \\ &= [\cos(2\pi f_i - 2\pi f_o)t - \cos(2\pi f_i + 2\pi f_o)t] \\ I_{LP}(t) &= \cos(2\pi f_i - 2\pi f_o)t \end{aligned} \quad (11)$$

$$\begin{aligned} Q(t) &= \sin(2\pi f_i t) \cdot 2\cos(2\pi f_o t) \\ &= [\sin(2\pi f_i - 2\pi f_o)t - \sin(2\pi f_i + 2\pi f_o)t] \\ Q_{LP}(t) &= \sin(2\pi f_i - 2\pi f_o)t \end{aligned} \quad (12)$$

The high frequency components $\sin(2\pi f_i + 2\pi f_o)t$ and $\cos(2\pi f_i + 2\pi f_o)t$ are filtered out

by the lowpass filters resulting in the last lines of Equation (11) and (12). The $I_{LP}(t)$ and $Q_{LP}(t)$ are sent to two separate ADC which after digitization become $I(n)$ and $Q(n)$. The $I(n)$ and $Q(n)$ are combined as $I(n)+jQ(n)$ for the FFT process.

Figure 5 shows the output samples from the I and Q channels after an 8 bit ADC. The input 1210 MHz sample signal is down converted to -20 MHz IF signal. The number of quantization levels of the ADC is $M=2^{n-1}=2^{8-1}=128$ (8 bit ADC is 7 bits plus sign) for the positive and negative cycles of the IF signals. After executing the FFTSHIFT function in MATLAB, the frequency information will be shifted back to 230 MHz.

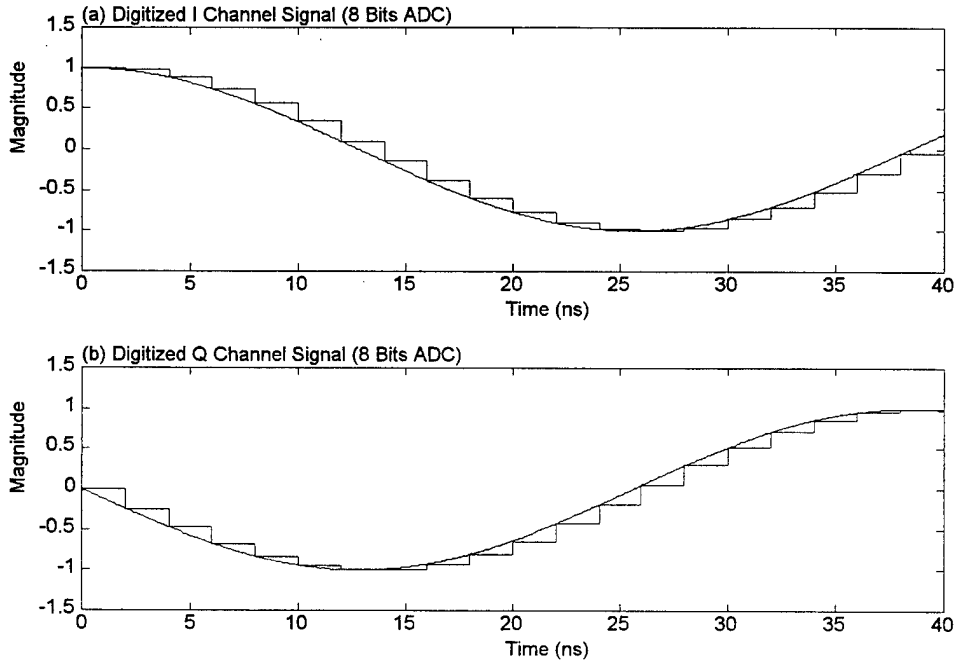


Figure 5 . ADC Output of a Digital Receiver with One Input Signal

Figure 6(a) shows a normalized IF spectrum of a digital ESM receiver using an 8 bit ADC and 512 sample FFT with one input signal at 230 MHz. The sampling rate for the ADC

is set to the Nyquist rate of 500 MHz. The data shown from sample 1 to sample 512 is for 500 MHz IF bandwidth. Since the amplitude of the carrier is a function of the converter's resolution in bits, normalizing the amplitude of the main frequency component to set the ideal full scale input level to 0 dB simplifies the evaluation and dBc means dB below carrier amplitude. We can use the normalized FFT results to find the peak noise level and determine the dynamic range of the receiver for a single input signal. Since there is only one input signal, there is no intermodulation distortion, but only the spurious response and quantization noise. Figure 6(b) shows the comparison of theoretical SNR and simulation results as a function of the number of ADC bits for one input signal. The simulation program for single signal analysis is listed in Appendix A.

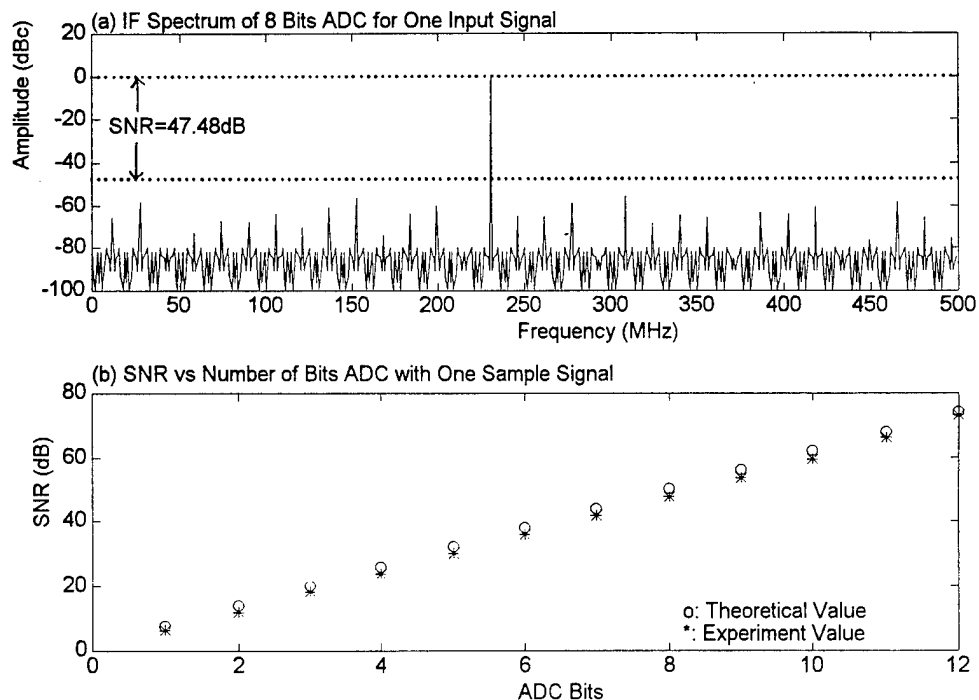


Figure 6 . IF Spectrum of a Digital Receiver with One Input Signal

Table 2 shows a comparison of the theoretical one input signal SNR and a computer simulation with results for different numbers of ADC bits for 230 MHz input signals. The simulation results for 230 MHz input signal are within 3dB from the ideal SNR values and increase at 6dB per bit.

Table 2. Theoretical SNR and Simulation SNR vs. Number of ADC Bits

ADC Bits	Ideal SNR (dB)	Simulation SNR (dB)
1	7.78	6.34
2	13.80	12.02
3	19.82	17.76
4	25.84	23.74
5	31.36	29.69
6	37.88	35.59
7	43.90	41.74
8	49.92	47.76
9	55.94	53.41
10	61.96	60.37
11	67.98	65.85
12	74.00	72.68

C. TWO SIGNALS ANALYSIS

Figure 7(a) shows the normalized output spectrum of a digital receiver with two 1 V peak amplitude sine wave signals $f_1=1230$ MHz and $f_2=1270$ MHz as the test signals. We can clearly see from the plot that there are ten equally separated inband intermodulation products generated by the two strong input signals which are the third ($2f_1-f_2$ and $2f_2-f_1$), fifth ($3f_1-2f_2$

and $3f_2-2f_1$), seventh ($4f_1-3f_2$ and $4f_2-3f_1$), ninth ($5f_1-4f_2$ and $5f_2-4f_1$), and eleventh ($6f_1-5f_2$ and $6f_2-5f_1$) order intermodulations whose amplitudes are higher than the peak noise level.

Figure 7(b) shows the comparison of ideal SNR and simulation results for different numbers of ADC bits.

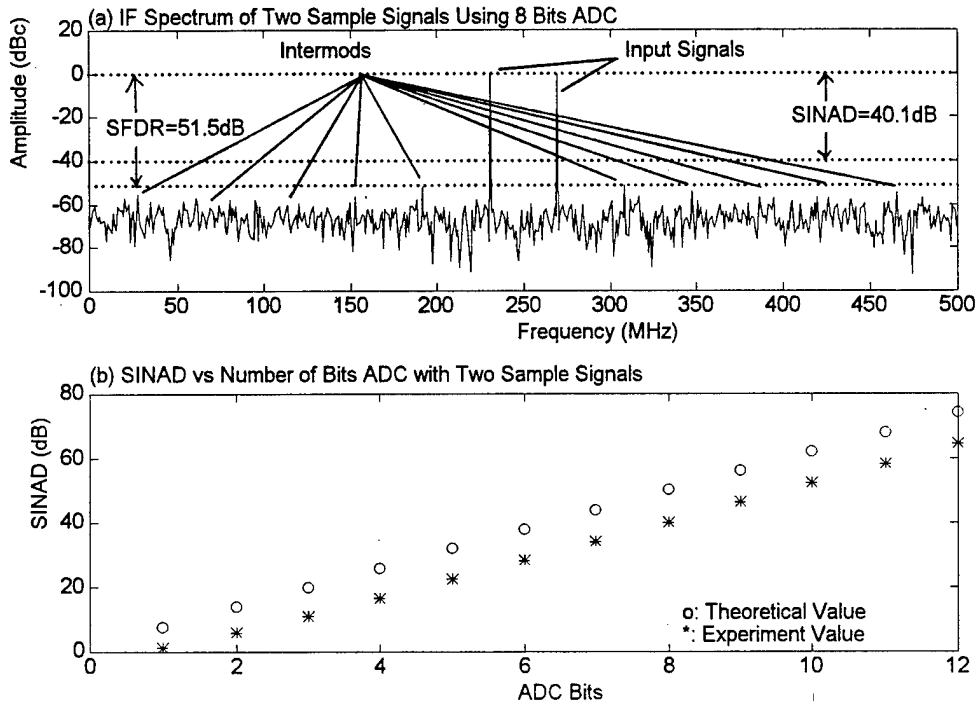


Figure 7. IF Spectrum of a Digital Receiver with Two Input Signals

Because of the intermodulation products, the SINAD obtained in this simulation is significantly worse than the theoretical SNR and the simulation result for a single signal SNR in the last section. The simulation program for two signals analysis is listed in Appendix B.

The intermodulation generated by the ADC results from the nonlinear quantization effects. Quantization introduces not only noise and distortion of the input signals, but also

generates intermodulation products from the two strong input signals. When the frequency spacing between f_1 and f_2 is smaller than the bandwidth of the receiver, the third order intermodulation becomes the principal source of spurious in band signals since it has the highest amplitude of all intermodulations. Figure 8 shows the quantized output samples of the I and Q channel ADCs for two input signals.

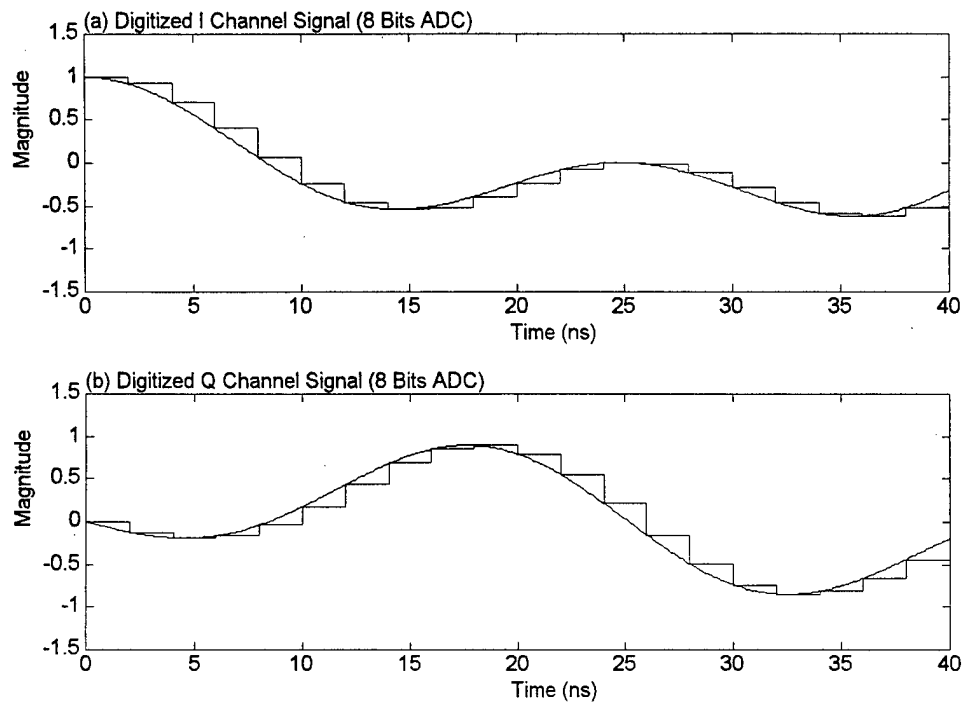


Figure 8 . ADC Output of a Digital Receiver with Two Input Signals

The dynamic range in this case refers to the two-signal or multiple signals analysis and is called the spurious free dynamic range (SFDR). SFDR is the most important specification in digital receiver design which determines the lowest distinguishable level of the input signals. As opposed to the sum of signum function used by Blachman [Ref. 14], the quantization

staircase output is represented by the sum of the input plus a sawtooth. Using an Fourier series for expanding the sawtooth, series expressions are obtained for the output quantized carriers and the resulting intermodulation products of any order. Blachman obtained an expression for the amplitude of the third-order and higher order intermodulation due to quantization. Because of the difficult mathematical integrations, only some special cases have been analyzed and further studies are required. Due to the complexity of Blachman approach, the procedure is not be followed in this thesis.

Table 3 shows the simulation results of SFDR, SINAD, and IMD for two input signals and verses the number of bits in the ADC. As expected, we can see that the intermodulation distortion decreases when the number of ADC bits increases.

Figure 9 shows two strong signals (210 MHz and 270 MHz) accompanied by a weak signal (230 MHz) whose amplitude appears between the third-order intermodulation and the peak noise level. The receiver does not recognize this weak signal as an input signal and tends to ignore it. Chapters III and IV will discuss methods of reducing intermodulation distortion and restoration of the weak signals.

Table 3. SFDR, SINAD, and IMD vs. Number of ADC Bits

ADC Bits	SFDR(dB)	SINAD(dB)	IMD(dBc)
1	9.75	1.26	-4.13
2	13.99	5.75	-8.83
3	20.03	10.95	-14.75
4	25.73	16.50	-20.30
5	32.69	22.34	-26.47
6	38.61	28.19	-32.54
7	45.12	34.13	-38.65
8	51.50	40.10	-44.63
9	57.78	46.11	-50.86
10	64.41	52.06	-57.24
11	71.08	58.24	-63.47
12	76.52	64.39	-69.79

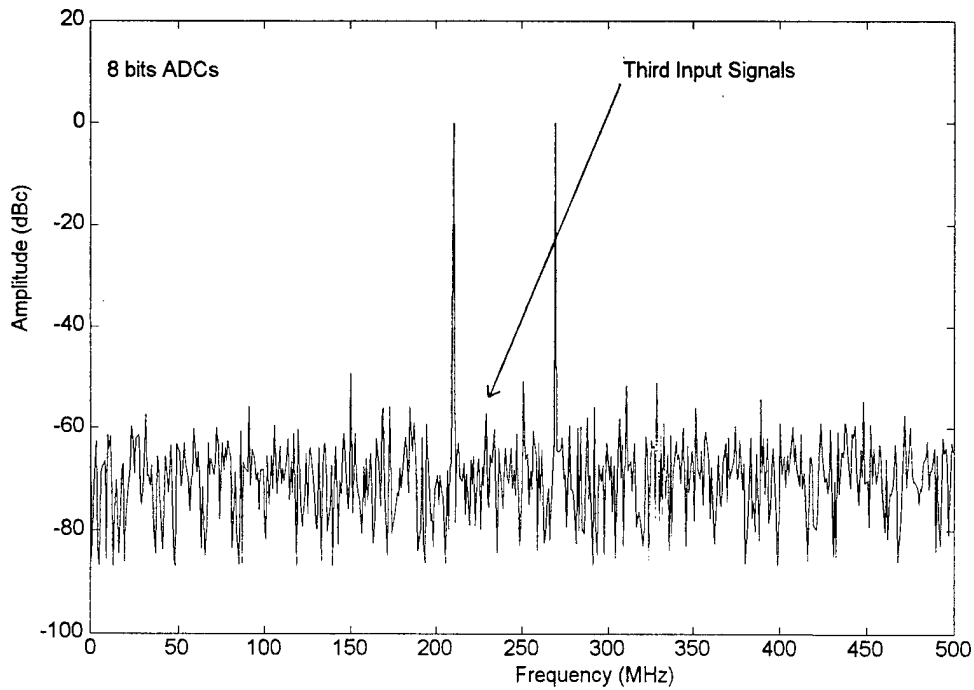


Figure 9 . A Third Input Signal Amplitude Below Peak Harmonic Level

D. MULTIPLE SIGNALS ANALYSIS

When multiple signals are applied to the input of an ADC, the output spectrum becomes unpredictable. Some intermodulation products tend to cancel with quantization noise resulting in amplitude reduction. The relationship between carriers and intermodulation products become uncertain when multiple signals are applied simultaneously to the receiver. The larger the number of input signals the worst the situation. In a real ESM environment, the reports from the receiver will be unreliable. Figure 10 shows the output spectrum of the ADC with fifteen sample signals and 8 bits quantization.

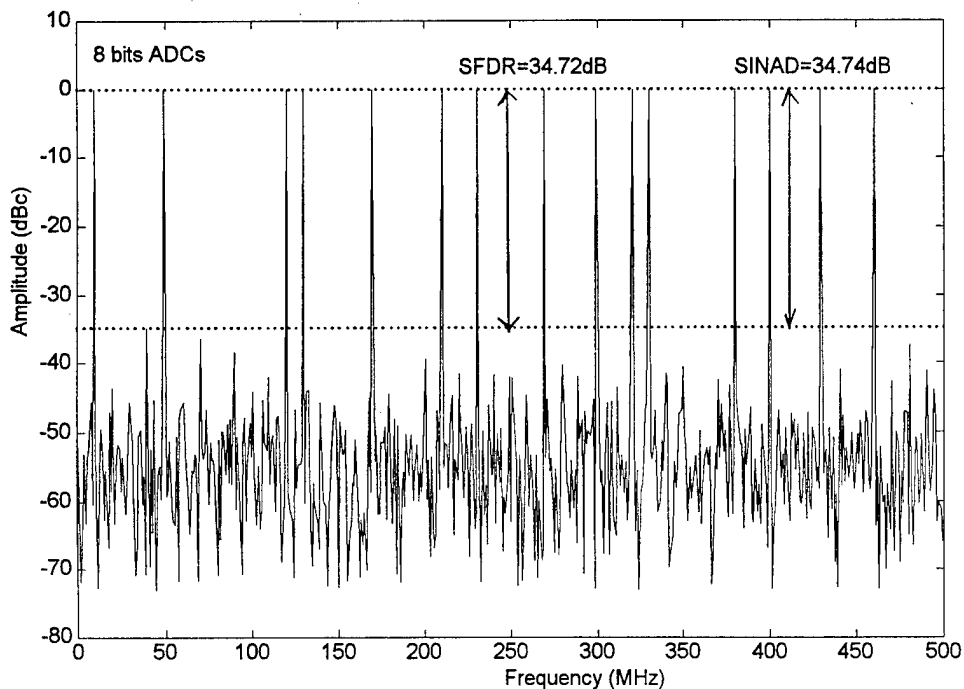


Figure 10. IF Spectrum of a Digital ESM Receiver with Fifteen Input Signals

When multiple signals are present, the number of intermodulation products becomes unpredictable and much smaller in amplitude when compared to Figure 10. Figure 10 clearly shows the frequency spacings between carriers and each intermodulation product as well as the amplitude of each intermodulation product. Table 4 lists the SFDR and SINAD of an 8 bit ADC for different numbers of input signals. We can see from the table that the SFDR and SINAD decrease as the number of input signals increase. As the number of input signals reached 15, the SFDR is almost equal to the SINAD.

Table 4. SFDR and SINAD of an 8 bits ADC

# of Signals	SFDR (dB)	SINAD (dB)
2	51.50	40.10
3	43.67	41.43
4	45.07	40.82
5	45.55	39.99
6	48.04	39.14
7	45.02	38.50
8	41.81	37.57
9	42.24	37.42
10	39.37	36.56
11	39.00	36.27
12	37.61	35.58
13	38.57	35.53
14	37.34	35.00
15	34.72	34.74

III. REDUCTION IN INTERMODULATION DISTORTION DUE TO ADDITIVE NOISE

When designing an analog receiver, the noise level is kept as low as possible in order to maintain a higher receiver sensitivity. In a digital ESM receiver, which uses an ADC as a crucial component, it is not necessary to follow this rule. Noise sometimes has a positive effect in an ADC as proposed by Tsui [Ref. 10] and Blachman [Ref. 15]. Noise may reduce the spurs generated by quantization. In fact, the effect of the noise is to smooth the nonlinear characteristic of the ADC. In general, the signal builds up by a factor of N for an N -point FFT with respect to noise. The FFT process has a gain of $10\log(N)$ dB for the coherent input signals and 0 dB for the noncoherent noise so adding noise to the digital receiver does not affect the amplitude of the carrier. Figure 11 shows the block diagram of a digital ESM receiver with a noise source added after the bandpass filter.

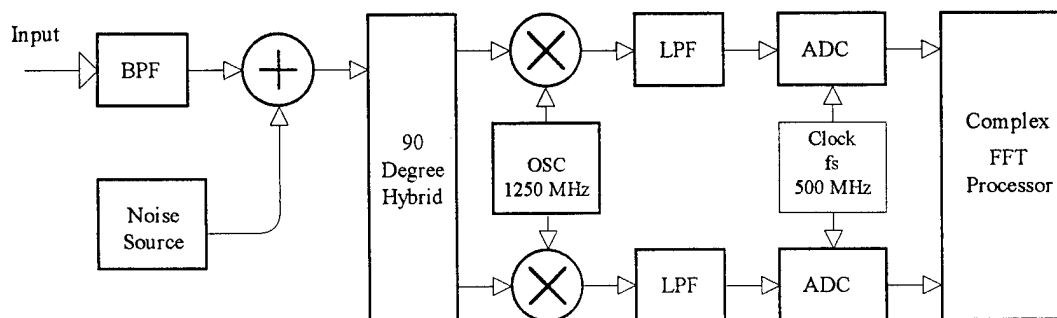


Figure 11. Block Diagram of a Digital ESM Receiver with a Noise Source

The digitization coherence will be reduced by the noise power as well as the intermodulation products. The intermodulation products may be reduced or even disappear

by controlling the additive noise level properly, but excess input noise power also reduces the SINAD level and reduces the SFDR of the digital ESM receiver.

The effect of adding noise to the input upon the distortion and intermodulation depends only on the probability distribution of the noise and is independent of its spectrum [Ref. 15]. The presence of a small amount of Gaussian wideband noise which is readily eliminated by a low pass filter, should cause the intermodulation products due to quantization to be undetectable.

A. ADDITIVE NOISE LEVEL AND INTERMODULATION DISTORTION

Figure 12 shows the comparison of the IF spectrums of the two input signals with and without additive noise. The two input signals are $f_1=1230$ MHz and $f_2=1270$ MHz and the ADCs use 8 bits. In Figure 12(a), we can observe the intermodulations between f_1 and f_2 . In Figure 12(b), we can see the amplitudes of the intermodulation products decrease resulting from -40 dBc additive noise. When adding noise to the input, the SFDR increases but also causes SINAD to decrease. Its a trade off between SFDR and SINAD.

There is no mathematical approach to obtain the optimum additive noise level for reducing the intermodulation products. In computer simulation, we can calculate the intermodulation distortion for different additive noise level and find the desired setting, but in practice we need to manually adjust the noise levels during intercepts.

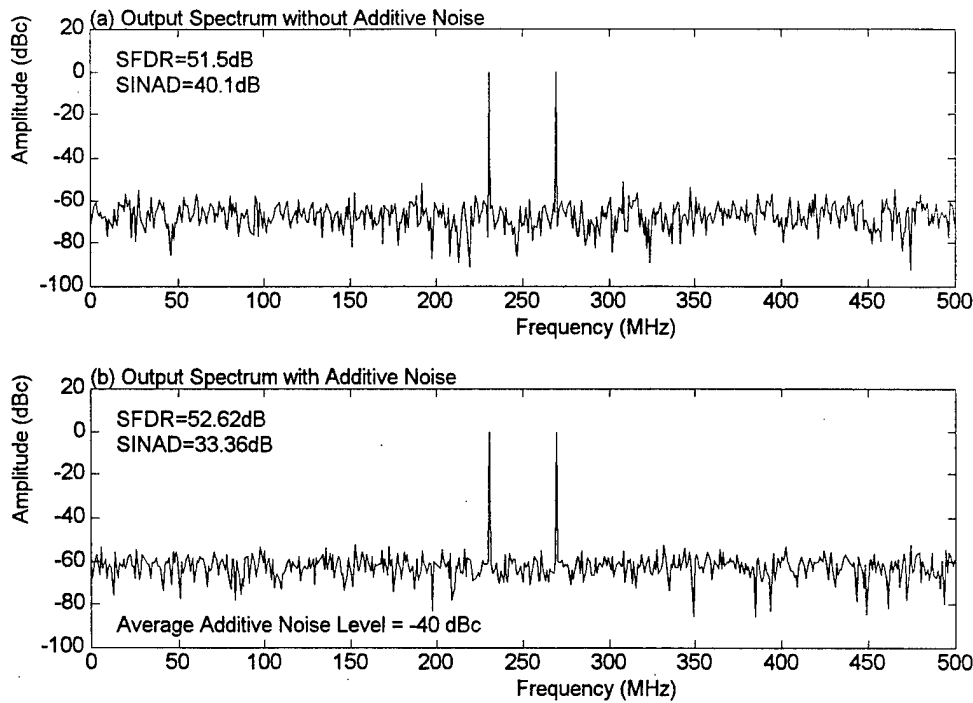


Figure 12. The Out Spectrum (a) with or (b) without Additive Noise

Figure 13 shows the relationship between additive noise level and intermodulation distortion of an 8 bit ADC for two input signals. The additive noise power starts from -140 dBc to 0 dBc for testing of two sample signals. When noise is added, the intermodulation distortion appears smaller until the noise power reaches -40 dBc, then all the intermodulation products become noise. The highest additive noise power for this simulation should be -40 dBc; levels higher than -40 dBc will have a negative effect on the receiver.

Figure 14 shows the relationship between the additive noise level and SINAD of an 8 bit ADC for two input signals. When noise is added, SINAD starts to decrease until the noise power is greater than -40 dBc, then the SINAD starts to drop drastically.

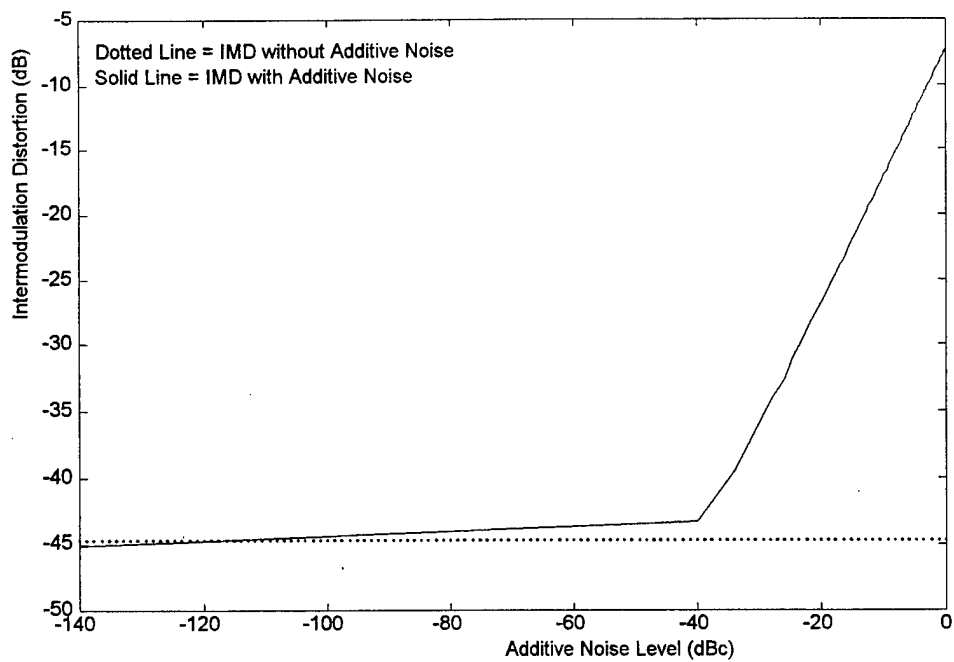


Figure 13. Additive Noise versus Intermodulation Distortion

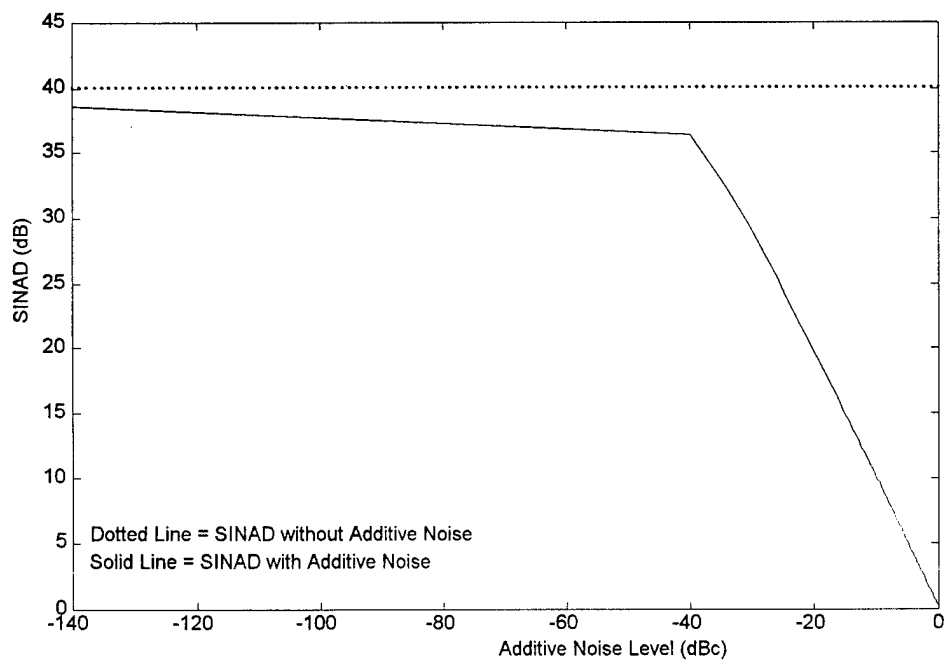


Figure 14. Additive Noise versus SINAD

B. ADDITIVE NOISE LEVEL AND SFDR

Figure 15 shows the relationship between additive noise level and SFDR of an 8 bit ADC for two input signals. When noise is added, the SFDR starts to increase until the noise power reaches -40 dBc, then the SFDR declines drastically. In comparison with the relationship between additive noise and intermodulation distortion and SINAD, the additive noise is most beneficial to the SFDR.

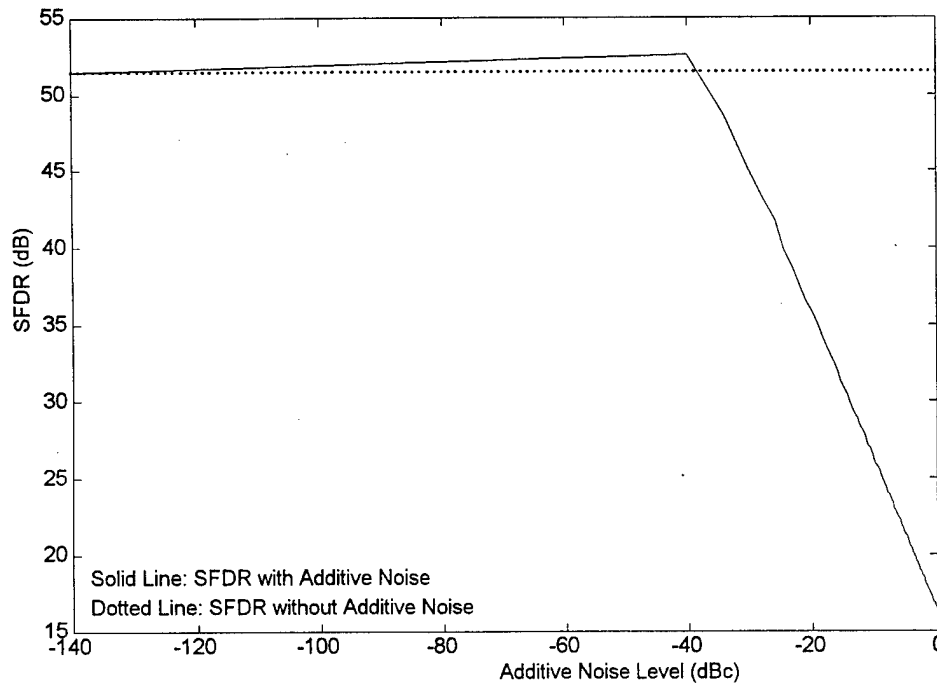


Figure 15. Additive Noise level verses SFDR

In order to test the SFDR after adding noise to the mixers, we can add a third input signal to the receiver to see if it is possible to restore the third signal from the intermodulation distortion. A third input signal $f_3=1240$ MHz is used to perform the test. The ADC is still

8 bits. The amplitude of the third input signal is set to -50 dBc for testing. We can see from Figure 16(a) that when a third input signal is added to the spectrum, it generates more spurious signals rather than the intermods.

By adding -40 dBc noise to the input, we can examine the amplitude of the third input signal which becomes higher than the third-order intermodulation products that are generated by f_1 and f_2 and all of the spurious signals disappear. Figure 16(b) shows that the amplitude of the third input signal now becomes greater than the third-order intermodulation products by the increased SFDR of the receiver. Again, there is no mathematical formula to specify the relationship between additive noise level and SFDR, but the noise does have a positive effect which increases the SFDR of the receiver by a small amount.

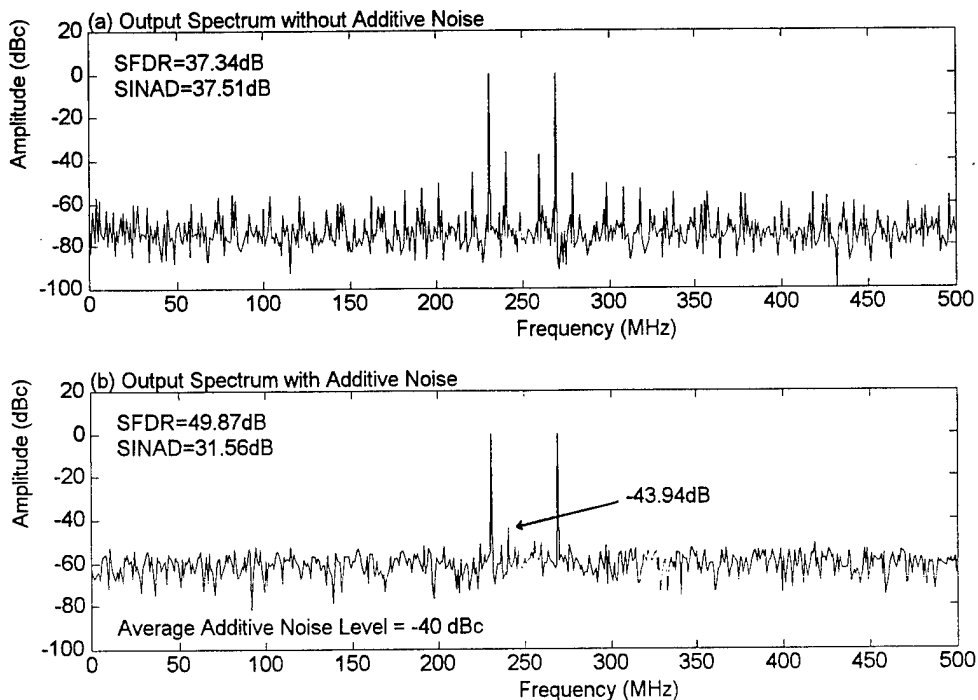


Figure 16 . SFDR Test with a Third Input Signal

IV. SUB-NYQUIST RATE APPROACH

In the previous chapter, we have seen how additive noise has the effect of reducing intermodulation distortion and increasing the SFDR, but the SFDR is still limited by the number of ADC bits unless we narrow the IF bandwidth in order to use an ADC with a larger number of bits to achieve higher dynamic range for the digital ESM receiver design. Narrowing the IF bandwidth means more receivers are needed in the system which makes the system more expensive and difficult to maintain.

An effective way to obtain a wide bandwidth with low sampling rate and larger number of ADC bits is to use sub-Nyquist rate sampling. The sub-Nyquist sampling scheme is very similar to the instantaneous frequency measurement (IFM) receiver. They both correlate the delayed and undelayed channel to obtain the frequency information.

Figure 17 shows the basic structure of a digital ESM receiver using the sub-Nyquist sampling approach. The digitized IF outputs are processed by the FFT operation. The FFT operation generates real and imaginary parts for the delayed and undelayed channels in the frequency domain.

Let $X_{ru}(k)$ and $X_{iu}(k)$ represent the real and imaginary parts of the undelayed channel, $X_{rd}(k)$ and $X_{id}(k)$ be the delayed channel, and τ is the delay time. The amplitude information can be calculated from the undelayed channel FFT output as:

$$X_u(k) = [X_{ru}(k)^2 + X_{iu}(k)^2]^{\frac{1}{2}} \quad (13)$$

and the frequency information can be calculated from the phase difference between the

delayed and undelayed channels.

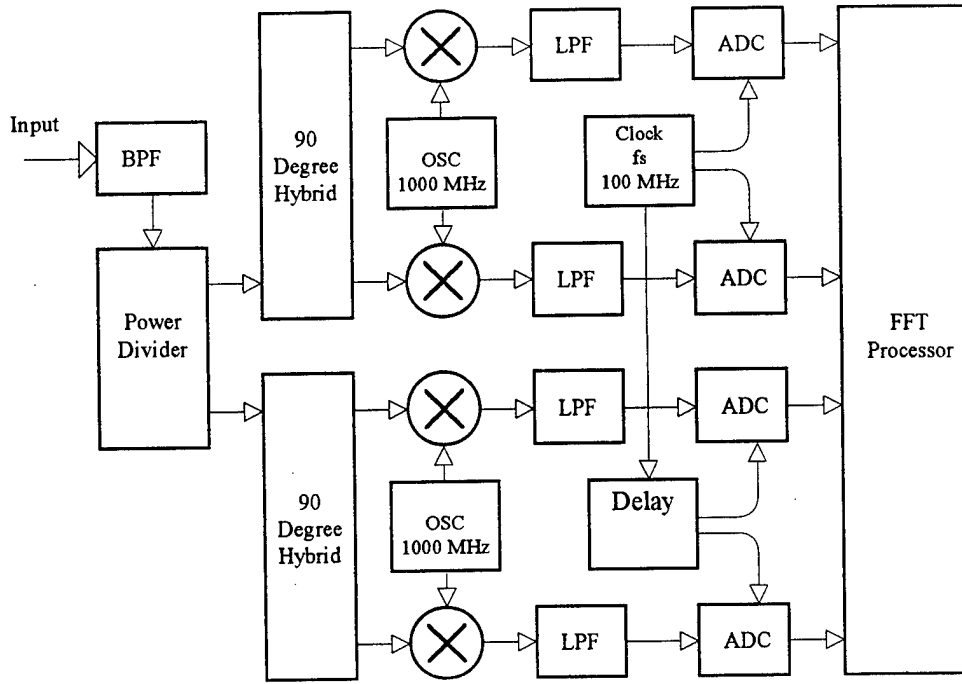


Figure 17. Basic Sub-Nyquist Sampling Structure of a Digital Receiver

Let θ_u be the phase of the undelayed channel and θ_d be the phase of the delayed channel. The frequency information can be calculated as follows:

$$\theta_u = \tan^{-1} \left[\frac{X_{iu}(k)}{X_{ru}(k)} \right] \quad (14)$$

$$\theta_d = \tan^{-1} \left[\frac{X_{id}(k)}{X_{rd}(k)} \right] \quad (15)$$

$$\Delta\theta = \theta_d - \theta_u = 2\pi\tau \quad (16)$$

$$f = \frac{\theta_d - \theta_u}{2\pi\tau} \quad (17)$$

The delay time τ determines the highest frequency as well as the bandwidth of the receiver (not the sampling rate f_s). When $\theta_r - \theta_u$ equals to 2π , the result in Equation (17) will be the highest frequency component from the FFT operation which represents the bandwidth of the receiver and has the following form:

$$\Delta B = f_{\max} = \frac{2\pi}{2\pi\tau} = \frac{1}{\tau} \quad (18)$$

Figure 18 shows the results of the sub-Nyquist rate simulation. The two input signals are 1230 MHz and 1270 MHz, the IF bandwidth is still 500 MHz, but the sampling rate is reduced to 100 MHz (1/10 Nyquist rate) to accommodate the sub-Nyquist rate scheme. The delay time setting for the delayed channel is 0.1ns. The maximum unambiguous bandwidth for the channelized digital ESM receiver can be derived from Equation (18) which is $\Delta B = 1/0.1\text{ns} = 10\text{ GHz}$. The sampling rate has been reduced to 100 MHz, thus, we can select a 12 bit ADC with 100 MHz bandwidth instead of using an 8 bit ADC with 1GHz bandwidth. The desired 500 MHz IF bandwidth will fit entirely into the 100 MHz bandwidth of the 12 bit ADC without ambiguity. An 8 bit 1GHz bandwidth ADC is also more expensive and has lower dynamic range than a 12 bit 100 MHz bandwidth ADC.

The input signals have been down converted to 230 MHz and 270 MHz by the mixers. From Figure 19, the IF signals are measured at 30 MHz and 70 MHz in the 100 MHz wide IF spectrum. Since the corresponding unambiguous frequency band of the channelized digital ESM receiver is 10 GHz, we do not know the exact frequencies of the two input signals because it can be 30 MHz and 70 MHz, 130 MHz and 170 MHz, 230 MHz and 270 MHz, 330 MHz and 370 MHz, 430 MHz and 470 MHz, ..., or 9930 MHz and 9970 MHz. By using

the phase calculation (Equation 17), we can obtain the true frequency information of the input signals correctly without ambiguity. A simulation program for the sub-Nyquist sampling scheme is listed in Appendix C.

The intermodulation distortion reduces when the input signals are the same as the previous simulation that used the Nyquist sampling rate, but intermodulation distortion does occur for some input signals. By adding noise to the input of this scheme, the intermodulation distortion can be reduced to an insignificant level.

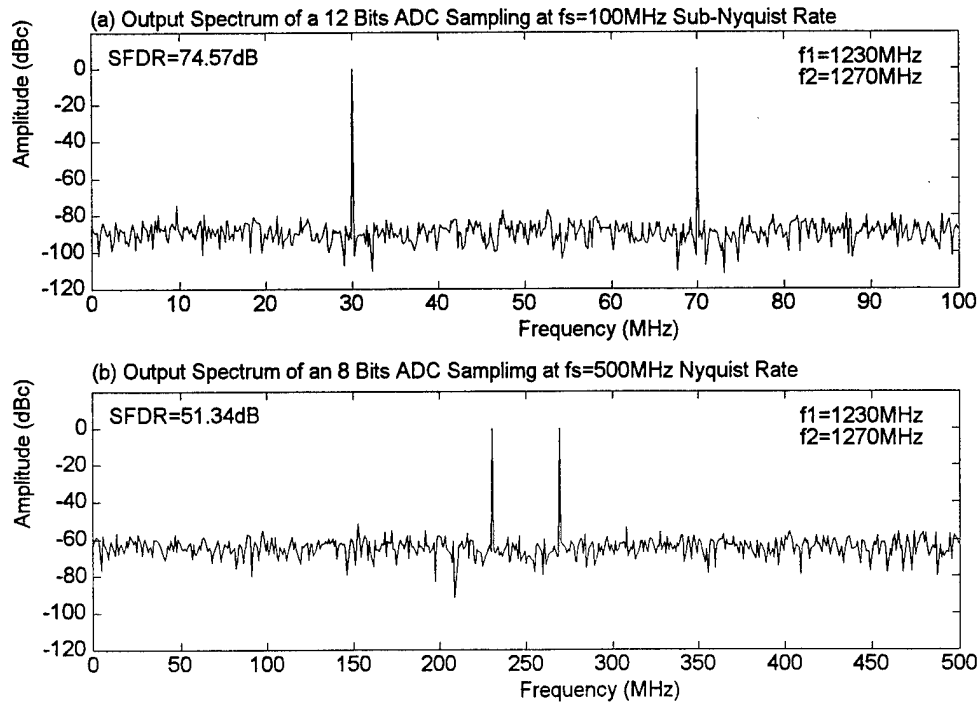


Figure 18. The Comparison of Sub-Nyquist and Nyquist Sampling Spectrum

Figure 19 shows the results when a 1240 MHz input signal is added to the receivers using a different number of bits for the ADCs. The amplitude of the third input signal is set

to -70.56 dB below the strongest amplitude of the carrier. Figure 19(a) shows a receiver using a 12 bit ADC with sub-Nyquist sampling rate; it is possible for the receiver to achieve a SFDR greater than 70 dB and detect the weak signal. In comparison to the sub-Nyquist scheme, Figure 19(b) shows a receiver using an 8 bit ADC with Nyquist sampling rate, the third input signal is too small to detect.

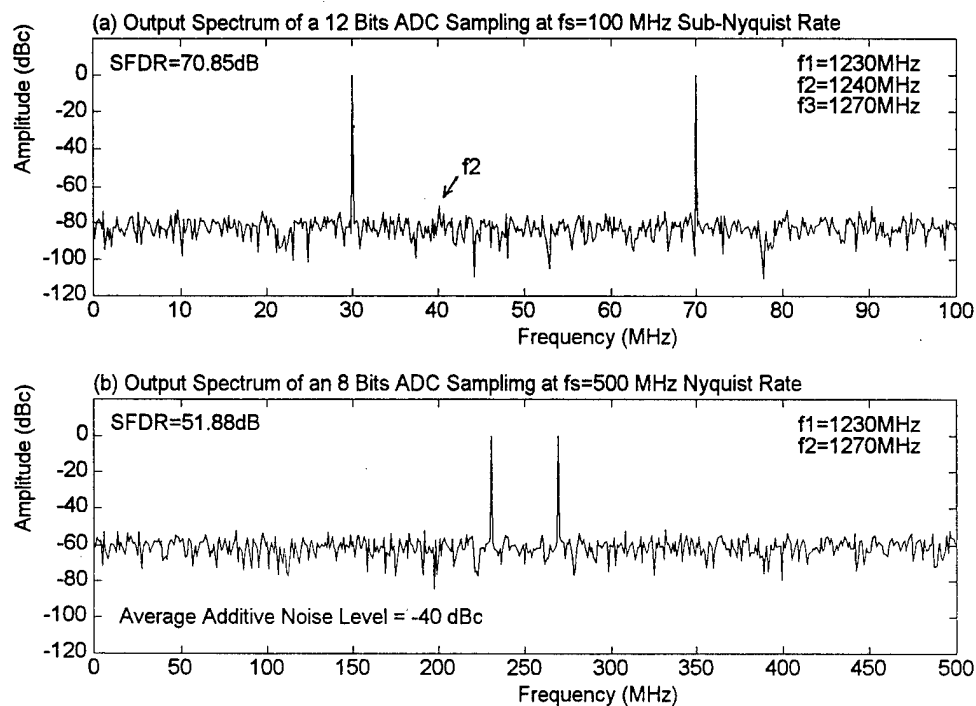


Figure 19 . SFDR Test for Two Different Sampling Schemes

V. CONCLUSION

This thesis has demonstrated how to utilize a noise source to reduce intermodulation distortion and increase the spurious free dynamic range of a channelized digital ESM receiver. This requires a wide bandwidth with resulting low dynamic range ADC to be used. In addition a sub-Nyquist sampling rate scheme was investigated which allows the full receiver bandwidth to be achieved with a smaller bandwidth but high dynamic range ADC. The data generated in this thesis are based on the selected frequencies of the input signals. Changing the frequency of the input signals results in slight variations of output data, but the principles remain the same.

It is desirable to build a receiver with a wide bandwidth (greater than 1 GHz) and a high dynamic range (above 70 dB) in order to process multiple signals at the same time. Limited by the current ADC technology, a channelized digital ESM receiver meeting these specifications appears to be beyond the state-of-the-art.

Although some spectrum estimation schemes such as sub-Nyquist rate sampling can achieve a wide bandwidth, it is unlikely to be used in real-time processing since they require intensive computation. It is difficult to achieve a wide bandwidth and high dynamic range in an ADC at the same time, but ADC technology is advancing at an astonishing speed, resulting in the digital receiver being a major trend of the future.

APPENDIX A

```
% TITLE: NYQUIST SAMPLING RATE SIMULATION FOR ONE INPUT SIGNAL
% SUBJECT: SIMULATION OF DIGITAL ESM RECEIVER SPECTRUM FOR ONE
%          INPUT SIGNAL USING FFT WITH TWO CHANNEL APPROACH
% PROGRAM: FIG06.M
```

```
clg;
clear;
fo=1.25e9;           % LOCAL OSCILLATOR FREQUENCY
fs=0.5e9;            % SAMPLING FREQUENCY FOR IF SIGNAL
fl=1.25e9;           % SAMPLE SIGNAL FREQUENCY #1
ifbw=0.5e9;          % IF BANDWIDTH
nfft=512;            % NUMBER OF FFT FOR IF BAND
N=8;                 % QUANTIZING BIT(S)
```

```
% GENERATE I(t) and Q(t) SIGNALS
```

```
dt=1/fs;             % SAMPLING TIME INTERVAL
t=0:dt:(nfft-1)*dt;  % SAMPLING PERIOD
fl=round(fl*nfft/fs)*(fs/nfft); % MATCHING INPUT FREQUENCY
It=cos(2*pi*(fl-fo)*t); % I CHANNEL SIGNALS
Qt=sin(2*pi*(fl-fo)*t); % Q CHANNEL SIGNALS
```

```
% QUANTIZATION PROCESS
```

```
M=2^(N-1);           % QUANTIZATION LEVELS
for I=1:nfft;
    xx(I)=M*It(I);
    yy(I)=M*Qt(I);
    if xx(I)>0;
        x(I)=ceil(xx(I))/M;
    else x(I)=floor(xx(I))/M;
    end;
    if yy(I)>0;
        y(I)=ceil(yy(I))/M;
    else y(I)=floor(yy(I))/M;
    end;
end;
sif=x+j*y;           % QUANTIZED TWO CHANNEL IF SIGNALS
```

```
% FIND FOURIER SPECTRUM OF THE IF SIGNALS
```

```

SIF=fft(sif,nfft);           % FFT OF QUANTIZED IF SIGNALS
SIF=fftshift(SIF);           % MOVE ZEROth LAG TO CENTER SPECTRUM
pif=SIF.*conj(SIF)/nfft;     % PSD OF QUANTIZED IF SIGNALS
PIF=pif/max(pif);            % NORMALIZED IF PSD OF SIGNALS
df=(fs/1e6)/nfft;           % FREQUENCY SPACING OF FFT POINTS
fx=0:df:(nfft-1)*df;        % SET INPUT SPECTRUM BANDWIDTH

```

% IF STAGE SPURIOUS SIGNALS

```

pifn=sort(PIF);
pifn(nfft)=[];
snr=10*log10(sum(pifn));     % SIGNAL TO NOISE RATIO
dr=10*log10(max(pifn));      % DYNAMIC RANGE

```

```

subplot(211),plot(fx,10*log10(PIF),grid;
text(0,26,'(a) IF Spectrum of 8 Bits ADC for One Sample Signal');
xlabel('Frequency (MHz)'),ylabel('Amplitude (dBc)');
axis([0 ifbw/1e6 -100 20]);
text(5,-30,['SNR=',num2str(-snr),'dB']);

```

% CALCULATIONS OF SFDR AND SINAD FOR DIFFERENT NUMBER OF BITS

```

bits=12;
for N=1:bits;
    M=2^(N-1);                % QUANTIZATION LEVELS
    for I=1:nfft;
        xx(I)=M*It(I);
        yy(I)=M*Qt(I);
        if xx(I)>0;
            x(I)=ceil(xx(I))/M;
        else x(I)=floor(xx(I))/M;
        end;
        if yy(I)>0;
            y(I)=ceil(yy(I))/M;
        else y(I)=floor(yy(I))/M;
        end;
    end;
    sif=x+j*y;

```

% FIND FOURIER SPECTRUM OF THE IF SIGNALS

```

SIF=fft(sif);                % FFT OF QUANTIZED IF SIGNALS
SIF=fftshift(SIF);           % MOVE ZEROth LAG TO CENTER SPECTRUM

```

```

pif=SIF.*conj(SIF)/nfft;    % PSD OF QUANTIZED IF SIGNALS
PIF=pif/max(pif);          % NORMALIZED IF PSD OF SIGNALS

```

```

% IF STAGE SPURIOUS SIGNALS

```

```

ifs=sort(PIF);
ifs(nfft)=[];
snr(N)=-10*log10(sum(ifs));
snrt(N)=1.76+6.02*N;
end;

N=1:bits;
subplot(212),plot(N,snrt,'o',N,snr,'*'),grid;
xlabel('ADC Bits'),ylabel('SNR (dB)');
text(6.2,12,'o: Theoretical Value');
text(6.2,5,'*: Experiment Value');
text(0,86,'(b) SNR for Different Number of Bits ADC with One Sample Signal');
fprintf('(a) SNR for Sample Signal ==>\n');
for N=1:bits;
    fprintf('%g Bits ADC ',N);
    fprintf('SNR = %1.2f dB\n',snr(N));
end;
fprintf('\n');
axis([0 bits 0 80]);

```


APPENDIX B

```
% TITLE: NYQUIST SAMPLING RATE SIMULATION FOR TWO INPUT %
          SIGNALS
% SUBJECT: SIMULATION OF DIGITAL ESM RECEIVER SPECTRUM FOR TWO
%          INPUT SIGNALS USING FFT WITH TWO CHANNEL APPROACH
% PROGRAM: FIG07.M
```

```
clc;
clear;
num=2;                % NUMBER OF SIGNALS
fo=1.25e9;            % LOCAL OSCILLATOR FREQUENCY
fs=0.5e9;             % SAMPLING FREQUENCY FOR IF SIGNAL
f1=1.23e9;            % SAMPLE SIGNAL FREQUENCY #1
f2=1.27e9;            % SAMPLE SIGNAL FREQUENCY #2
ifbw=0.5e9;           % IF BANDWIDTH
nfft=512;             % NUMBER OF FFT FOR IF BAND
N=8;                  % QUANTIZING BIT(S)
```

```
% GENERATE I(t) and Q(t) SIGNALS
```

```
dt=1/fs;              % SAMPLING TIME INTERVAL
t=0:dt:(nfft-1)*dt;   % SAMPLING PERIOD
f1=round(f1*nfft/fs)*(fs/nfft); % MATCHING INPUT FREQUENCY
f2=round(f2*nfft/fs)*(fs/nfft); % WITH FFT RESOLUTION
It=cos(2*pi*(f1-fo)*t)+cos(2*pi*(f2-fo)*t);
Qt=sin(2*pi*(f1-fo)*t)+sin(2*pi*(f2-fo)*t);
```

```
% QUANTIZATION PROCESS
```

```
M=2^(N-1);           % QUANTIZATION LEVELS
for I=1:nfft;
    xx(I)=(M*It(I))/num;
    yy(I)=(M*Qt(I))/num;
    if xx(I)>0;
        x(I)=ceil(xx(I))/M;
    else x(I)=floor(xx(I))/M;
    end;
    if yy(I)>0;
        y(I)=ceil(yy(I))/M;
    else y(I)=floor(yy(I))/M;
    end;
```

```

end;
sif=x+j*y; % QUANTIZED TWO CHANNEL IF SIGNALS

% FIND FOURIER SPECTRUM OF THE IF SIGNALS

SIF=fft(sif,nfft); % FFT OF QUANTIZED IF SIGNALS
SIF=fftshift(SIF); % MOVE ZERO TH LAG TO CENTER SPECTRUM
pif=SIF.*conj(SIF)/nfft; % PSD OF QUANTIZED IF SIGNALS
PIF=pif/max(pif); % NORMALIZED IF PSD OF SIGNALS
df=(fs/1e6)/nfft; % FREQUENCY SPACING OF FFT POINTS
fx=0:df:(nfft-1)*df; % SET INPUT SPECTRUM BANDWIDTH

% IF STAGE SPURIOUS SIGNALS

pifn=sort(PIF);
signal=pifn(nfft-num+1:nfft) % SIGNAL POWER
pifn(nfft-num+1:nfft)=[];
IMD=10*log10(sum(pifn(nfft-num-10+1:nfft-num)))
sinad=10*log10(sum(signal)/sum(pifn)); % SIGNAL TO NOISE AND DISTORTIONS
sfdr=10*log10(max(pifn)); % SPURIOUS FREE DYNAMIC RANGE

subplot(211),plot(fx,10*log10(PIF)),grid;
text(0,26,'(a) IF Spectrum of 8 Bits ADC for Two Sample Signals');
xlabel('Frequency (MHz)'),ylabel('Amplitude (dBc)');
axis([0 fs/1e6 -100 20]);
text(405,-30,['SINAD=',num2str(sinad),'dB']);
text(10,-30,['SFDR=',num2str(-sfdr),'dB']);
text(310,10,'Input Signals','sc');
text(110,10,'Intermods','sc');

% CALCULATIONS OF SFDR AND SINAD FOR DIFFERENT NUMBER OF BITS

bits=12;
for N=1:bits;
    M=2^(N-1); % QUANTIZATION LEVELS
    for I=1:nfft;
        xx(I)=(M*It(I))/num;
        yy(I)=(M*Qt(I))/num;
        if xx(I)>0;
            x(I)=ceil(xx(I))/M;
        else x(I)=floor(xx(I))/M;
        end;
        if yy(I)>0;

```

```

y(I)=ceil(yy(I))/M;
else y(I)=floor(yy(I))/M;
end;
end;
sif=x+j*y;

```

% FIND FOURIER SPECTRUM OF THE IF SIGNALS

```

SIF=fft(sif);           % FFT OF QUANTIZED IF SIGNALS
SIF=fftshift(SIF);      % MOVE ZERO TH LAG TO CENTER SPECTRUM
pif=SIF.*conj(SIF)/nfft; % PSD OF QUANTIZED IF SIGNALS
PIF=pif/max(pif);       % NORMALIZED IF PSD OF SIGNALS

```

% IF STAGE SPURIOUS SIGNALS

```

ifs=sort(PIF);
signal=ifs(nfft-num+1:nfft); % SIGNAL POWER
ifs(nfft-num+1:nfft)=[];
sinad(N)=10*log10(sum(signal)/sum(ifs));
snrt(N)=1.76+6.02*N;
end;

```

```

N=1:bits;
subplot(212),plot(N,snrt,'o',N,sinad,'*'),grid;
xlabel('ADC Bits'),ylabel('SINAD (dB)');
text(6.2,12,'o: Theoretical Value');
text(6.2,5,'*: Experiment Value');
text(0.86,'(b) SINAD for Different Number of Bits ADC with Two Sample Signals');
fprintf('(a) SINAD for Sample Signal ==>\n');
for N=1:bits;
    fprintf('%g Bits ADC ',N);
    fprintf('SINAD = %1.2f dB\n',sinad(N));
end;
fprintf('\n');

```


APPENDIX C

```
% TITLE: SUB-NYQUIST SAMPLING RATE SIMULATION FOR TWO
%         INPUT SIGNALS
% SUBJECT: SIMULATION OF DIGITAL ESM RECEIVER SPECTRUM
%         USING SUB-NYQUIST RATE WITH TWO CHANNEL APPROACH
% PROGRAM: FIG18.M
```

```
clear;
num=2; % NUMBER OF SIGNALS
fo=1.25e9; % LOCAL OSCILLATOR FREQUENCY
fs1=0.1e9; % SUB-NYQUIST SAMPLING FREQUENCY
fs2=0.5e9; % NYQUIST SAMPLING FREQUENCY
f1=1.23e9; % SAMPLE SIGNAL FREQUENCY #1
f2=1.27e9; % SAMPLE SIGNAL FREQUENCY #2
ratio=1; % RATIO OF SIGNAL #1 AND #2
Tao=0.1e-9; % DELAY TIME FOR DELAYED CHANNEL
nfft=512; % NUMBER OF FFT
N=12; % QUANTIZING BIT(S)
```

```
% GENERATE EXTERNAL NOISE
```

```
load noise.dat;
Noise=0.001*noise'; % SET NOISE LEVEL
if nfft<2048
    Noise(nfft+1:2048)=[];
end;
```

```
% PART I: SIMULATION OF ADC USING SUB-NYQUIST SAMPLING RATE
```

```
dt=1/fs1; % SAMPLING TIME INTERVAL
t=dt:dt:nfft*dt; % SAMPLING PERIOD
td=dt-Tao:dt:nfft*dt-Tao; % SAMPLING PERIOD FOR DELAYED CHANNEL
```

```
% GENERATE INPUT SIGNALS s(t)
```

```
f1=round(f1*nfft/fs1)*(fs1/nfft); % MATCHING INPUT FREQUENCY
f2=round(f2*nfft/fs1)*(fs1/nfft); % WITH FFT RESOLUTION
st1=sin(2*pi*f1*t); % SINUSOIDAL INPUT SIGNAL #1
st2=ratio*sin(2*pi*f2*t); % SINUSOIDAL INPUT SIGNAL #2
st=st1+st2; % SINUSOIDAL INPUT SIGNALS
std1=sin(2*pi*f1*td); % SINUSOIDAL INPUT SIGNAL #1
```

```

std2=ratio*sin(2*pi*f2*td);          % SINUSOIDAL INPUT SIGNAL #2
std=std1+std2;                       % DELAYED SINUSOIDAL INPUT SIGNALS
SIGNAL=sum(st1.^2)+sum(st2.^2);
NOISE=sum(Noise.^2);
SNR=10*log10(SIGNAL/NOISE)
It=cos(2*pi*(f1-fo)*t)+ratio*cos(2*pi*(f2-fo)*t); % UNDELAYED I CHANNEL
Qt=sin(2*pi*(f1-fo)*t)+ratio*sin(2*pi*(f2-fo)*t); % UNDELAYED Q CHANNEL
Itd=cos(2*pi*(f1-fo)*td)+ratio*cos(2*pi*(f2-fo)*td); % DELAYED I CHANNEL
Qtd=sin(2*pi*(f1-fo)*td)+ratio*sin(2*pi*(f2-fo)*td); % DELAYED Q CHANNEL

% QUANTIZATION PROCESS

M=2^(N-1);                          % QUANTIZATION LEVELS
for I=1:nfft;
    xx(I)=(M*It(I))/num;
    yy(I)=(M*Qt(I))/num;
    xxd(I)=(M*Itd(I))/num;
    yyd(I)=(M*Qtd(I))/num;
    if xx(I)>0;
        x(I)=ceil(xx(I))/M;
    else x(I)=floor(xx(I))/M;
    end;
    if yy(I)>0;
        y(I)=ceil(yy(I))/M;
    else y(I)=floor(yy(I))/M;
    end;
    if xxd(I)>0;
        xd(I)=ceil(xxd(I))/M;
    else xd(I)=floor(xxd(I))/M;
    end;
    if yyd(I)>0;
        yd(I)=ceil(yyd(I))/M;
    else yd(I)=floor(yyd(I))/M;
    end;
end;
sif=x+j*y;                          % QUANTIZED UNDELAYED CHANNEL IF SIGNALS
sifd=xd+j*yd;                       % QUANTIZED DELAYED CHANNEL IF SIGNALS

% FIND FOURIER SPECTRUM OF THE IF SIGNALS

SIF=fft(sif,nfft);                  % FFT OF QUANTIZED IF SIGNALS
SIFd=fft(sifd,nfft);                % FFT OF QUANTIZED IF SIGNALS
psd=abs(SIF);                       % OUTPUT AMPLITUDE

```

```

PSD=psd/max(psd);           % NORMALIZED IF PSD OF SIGNALS
df=(fs1/1e6)/nfft;          % FREQUENCY SPACING OF FFT POINTS
fx=0:df:(nfft-1)*df;        % SET INPUT SPECTRUM BANDWIDTH

subplot(211),plot(fx,20*log10(PSD)),grid;
text(0,8,'(a) Output Spectrum of a 12 Bits ADC Sampling at fs=100MHz Sub-Nyquist
Rate','sc');
xlabel('Frequency (MHz)'),ylabel('Amplitude (dBc)');
axis([0 fs1/1e6 -120 20]);

```

% IF STAGE SPURIOUS SIGNALS

```

PSDN=sort(PSD);
PSDN(nfft-num+1:nfft)=[];
SFDR=-20*log10(max(PSDN));   % MAX SPUR LEVEL
No=1;
for m=1:nfft;
    if PSD(m)>max(PSDN)
        Tu=atan(imag(SIF(m))/real(SIF(m)));
        Td=atan(imag(SIFd(m))/real(SIFd(m)));
        Freq=round(abs((Td-Tu)/(2*pi*Tao))/1e6);
        fprintf('Input Signal %g',No);
        fprintf(' = %g MHz\n',Freq+1e3);
        f(No)=Freq+1e3;
        No=No+1;
    end;
end;
text(82,5,['f1=',num2str(f(1)),'MHz'],'sc');
text(82,-6,['f2=',num2str(f(2)),'MHz'],'sc');
text(2,5,['SFDR=',num2str(SFDR),'dB'],'sc');

```

% PART II: SIMULATION OF ADC USING NYQUIST SAMPLING RATE

```

N=8;
dt=1/fs2;           % SAMPLING TIME INTERVAL
t=0:dt:(nfft-1)*dt; % SAMPLING PERIOD

```

% GENERATE INPUT SIGNALS s(t)

```

f1=round(f1*nfft/fs2)*(fs2/nfft); % MATCHING INPUT FREQUENCY
f2=round(f2*nfft/fs2)*(fs2/nfft); % WITH FFT RESOLUTION
It=cos(2*pi*(f1-fo)*t)+ratio*cos(2*pi*(f2-fo)*t)+Noise; % I CHANNEL SIGNALS
Qt=sin(2*pi*(f1-fo)*t)+ratio*sin(2*pi*(f2-fo)*t)+Noise; % Q CHANNEL SIGNALS

```

% QUANTIZATION PROCESS

```
M=2^(N-1);                                % QUANTIZATION LEVELS
for I=1:nfft;
    xx(I)=(M*It(I))/num;
    yy(I)=(M*Qt(I))/num;
    if xx(I)>0;
        x(I)=ceil(xx(I))/M;
    else x(I)=floor(xx(I))/M;
    end;
    if yy(I)>0;
        y(I)=ceil(yy(I))/M;
    else y(I)=floor(yy(I))/M;
    end;
end;
sif=x+j*y;                                % QUANTIZED TWO CHANNEL IF SIGNALS
```

% FIND FOURIER SPECTRUM OF THE IF SIGNALS

```
SIF=fft(sif,nfft);                        % FFT OF QUANTIZED IF SIGNALS
SIF=fftshift(SIF);                        % MOVE ZERO TH LAG TO CENTER SPECTRUM
pif=SIF.*conj(SIF)/nfft;                  % PSD OF QUANTIZED IF SIGNALS
PIF=pif/max(pif);                         % NORMALIZED IF PSD OF SIGNALS
df=(fs/2/1e6)/nfft;                      % FREQUENCY SPACING OF FFT POINTS
fx=0:df:(nfft-1)*df;                     % SET INPUT SPECTRUM BANDWIDTH
```

```
subplot(212),plot(fx,10*log10(PIF)),grid;
text(0,8,'(b) Output Spectrum of an 8 Bits ADC Sampling at fs=500MHz Nyquist
Rate','sc');
xlabel('Frequency (MHz)'),ylabel('Amplitude (dBc)');
axis([0 fs/2/1e6 -120 20]);
```

% IF STAGE SPURIOUS SIGNALS

```
pifn=sort(PIF);
pifn(nfft-num+1:nfft)=[];
SFDR=-10*log10(max(pifn));
f1=round(f1/1e7)*10;
f2=round(f2/1e7)*10;
text(10,6,['SFDR=',num2str(SFDR),'dB'],'sc');
text(410,5,['f1=',num2str(f1),'MHz'],'sc');
text(410,-6,['f2=',num2str(f2),'MHz'],'sc');
```

LIST OF REFERENCES

1. Schleher, D. C., *Introduction to Electronic Warfare*. Artech House, Inc., 1986.
2. Walden, R. Hughes Research Laboratories, Malibu, CA, Private Communication.
3. Wang, K.C. Science Center, Rockwell International, Thousand Oaks, CA, Private Communication.
4. Spaanewburg, H. Honeywell Inc., Bloomington, MN, Private communication.
5. Lemnios, Z. Advanced Research Projects Agency, Arlington, VA, Private communication.
6. IEWD, "Wideband ADC, " Rome Laboratory, Nov., 1994.
7. M&AE1995 Product Intelligence, "14-bit A-D converters have what it takes," *Military & Aerospace Electronics*, pp. s4-s6, Feb., 1995.
8. Frank, G., "12-Bit IC ADCs Relieve Error Budgets," *Electronic Design*, pp. 57-63, Oct., 1995.
9. Product Technology, "Fast ADC Grabs 1GSamples over 900-MHz Bandwidth," *Microwaves & RF*, p.136, May, 1995.
10. Product Technology, "SiGe ADC Powers Direct-Sampled Receivers," *Microwaves & RF*, p. 153, April, 1996.
11. Tsui, J., *Digital Techniques for Wideband Receivers*, Artech House, Inc., 1995.
12. Peot, M. A., "Electronic Warfare Signal Processing in the Year 2000," *EW Design Engineers' Handbook*, Horizon House-Microwave, Inc., 1989.
13. Mielke, J. A., "Frequency Domain Testing of ADCs." *IEEE Design & Test of Computers*, Spring, 1996.
14. Blachman, N.M., "Third-Order Intermodulation due to quantization," *IEEE Trans. Commun.*, vol. Com-29, pp. 1386-1389, 1981.
15. Blachman, N.M., "Intermodulation and Distortion due to Quantization of Sinusoids," *IEEE Trans. Acoust., Speech, Signal Processing*, vol. ASSP-33 Dec., 1985.

INITIAL DISTRIBUTION LIST

	No. Copies
1. Defense Technical Information Center 8725 Kingman Rd., Ste 0944 Ft. Belvoir, VA 22060-6218	2
2. Dudley Knox Library Naval Postgraduate School 411 Dyer Rd. Monterey, CA 93943-5101	2
3. Chairman F. Levien, Code EW Department of Electronic Warfare Naval Postgraduate school Monterey, CA 93943	1
4. Professor D.C. Schleher, Code EW/Sc Department of Electronic Warfare Naval Postgraduate School Monterey, CA 93943	1
5. Professor David Jenn, Code EC/Jn Department of Electrical and Computer Engineering Naval Postgraduate School Monterey, CA 93943	1
6. Ming-Jen Cheng 3-3, Lane 193, Yuan-Yuan Road, Nuan-Nuan Ward, Keelung, Taiwan, R. O. C.	2